

# Review of material and flexural overstrength factors for Grade 300E reinforcing steel used in New Zealand

S. Davies-Colley<sup>1</sup>, B. Kleinjan<sup>1</sup>, D.K. Bull<sup>1,2</sup> & G.J. Morris<sup>1</sup>

<sup>1</sup>Department of Civil and Natural Resources Engineering, University of Canterbury, Christchurch, New Zealand

<sup>2</sup>Holmes Consulting Group, New Zealand



2015 NZSEE  
Conference

**ABSTRACT:** Recent research suggests that a material overstrength factor of 1.25 for Grade 300E reinforcing steel is too low. The accuracy of overstrength factors is critical for designing ductile reinforced concrete (RC) structures according to capacity design principles. In order to review the overstrength characteristics, this research uses tension test data from a range of Grade 300E reinforcing steel samples supplied by Pacific Steel. A moment-curvature analysis tool was developed to analyse the flexural and material overstrength factors for a range of RC sections. The variables and assumptions defining the models and sections used in this analysis tool are discussed within. Grade 300E reinforcing steel was found to have significant strain hardening properties which subsequently produces large flexural overstrength factors. The results from 7176 section analyses agree with previous studies in that the material overstrength factor stated in the NZ Concrete Structures Standard, NZS3101:2006, needs to be increased from 1.25.

## 1 INTRODUCTION

Modern well-designed reinforced concrete (RC) structures are designed according to capacity design principles in which a strength hierarchy is established to promote ductile failure mechanisms in the structure, typically known as ‘plastic hinging’, during severe seismic actions. Less desirable brittle mechanisms are prevented by considering the maximum feasible strength of potential plastic hinge regions. In structural design practice, the strength hierarchy is achieved using an overstrength factor to define the maximum capacity a member may reach beyond the nominal design capacity. The overstrength factor must allow for strength enhancements affected by the ‘likely maximum material strength’ of the reinforcing steel and concrete that exceeds the nominal design strength. Grade 300E reinforcing steel is currently used as a standard grade in New Zealand (NZ) in the construction of RC structures. Grade 300E reinforcing steel has a 5th percentile characteristic yield strength,  $f_y$ , of 300 MPa. The stress-strain behaviour of this reinforcing steel is expected to have a significant influence on the overstrength capacity of ductile RC structural components.

This paper reviews some previous studies on overstrength, followed by details regarding the development of the moment-curvature sectional analysis tool ‘*MC analysis*’ to evaluate the flexural overstrength factor,  $\lambda_o$ , and the material overstrength factor,  $\phi_{o,fy}$ , of Grade 300E reinforcing steel. Tension test data of Grade 300E reinforcing steel samples (supplied by Pacific Steel) were analysed in a range of RC sections. Different variables and assumptions of the models used in the analysis are also discussed within.

## 2 HISTORICAL STUDIES

Grade 300E and 500E reinforcing steel are the only two grades of reinforcing steel currently used in NZ construction. In the past, Grade 275 and Grade 380 was the predominant grade for reinforcing steel. Andriano and Park (1986) conducted the first notable study on overstrength to determine the “probable stress-strain properties” of both Grade 275 and 380 by utilising older Pacific Steel test data and Monte Carlo simulation techniques. The outcomes of that study suggested that flexural overstrength factors,  $\lambda_o$ , for the Grade 275 and 380 to be 1.25 and 1.40, respectively, and were adopted in the 1982 NZ Concrete Structures Standard (NZS 3101:1982).

During the 1995 revision of NZS 3101, the commercially available reinforcing steel was either Grade 300E or Grade 430. The introduction of “E grade” steel was the industry’s recognition of ductile seismic (Earthquake) grade reinforcing steel with a minimum elongation of 15% at maximum tensile strength. Grade 300E steel has the same metallurgical composition as Grade 275, while Grade 430 had improved ductility and reduced strain hardening. The overstrength factor for both steel grades was taken as 1.25 in NZS3101:1995. Later in 2001, Grade 430 was replaced with Grade 500E steel and the corresponding flexural overstrength factor was amended to 1.40. Following the outcomes of an analytical study by Bull and Allington (2003) on 1600 stress-strain curves from Pacific Steel, the factor was revised to 1.35.

In NZS3101:2006 (Amendment 2), the specified material overstrength factors,  $\phi_{o,fy}$ , were 1.25 for Grade 300E steel, and 1.35 for Grade 500E steel, respectively. A recent experimental study by Brooke and Ingham (2011) of 100 beam-column joint specimens concluded the same overstrength factor should be applied to both grades of steel. They recommend that an appropriate material overstrength factor is between 1.35 and 1.40 for Grade 300E reinforcing steel.

### 3 VARIABLES INVESTIGATED

#### 3.1 Reinforcing steel model from Grade 300E tension test data

The modelled reinforcing steel properties were based on direct tension tests carried out by Pacific Steel during 2013 and 2014 on the Grade 300E deformed bars for a range of bar diameters. The stress-strain model used to represent the actual steel behaviour was developed by Mander (1984). An assumption of this model is that the stress-strain relationship is the same in compression and tension. The actual compressive behaviour of the steel is somewhat of an approximation as strain softening and longitudinal bar buckling is not accounted for. Strain softening and bar buckling would decrease the strength of the RC component, although these factors were neglected for the purpose of this study as overstrength factors are used to consider the maximum possible strength. It is also assumed that RC members are well detailed with adequate transverse reinforcement in accordance with NZS3101:2006 so that bar buckling is mitigated. The properties required to define the model are shown in Figure 1(a).

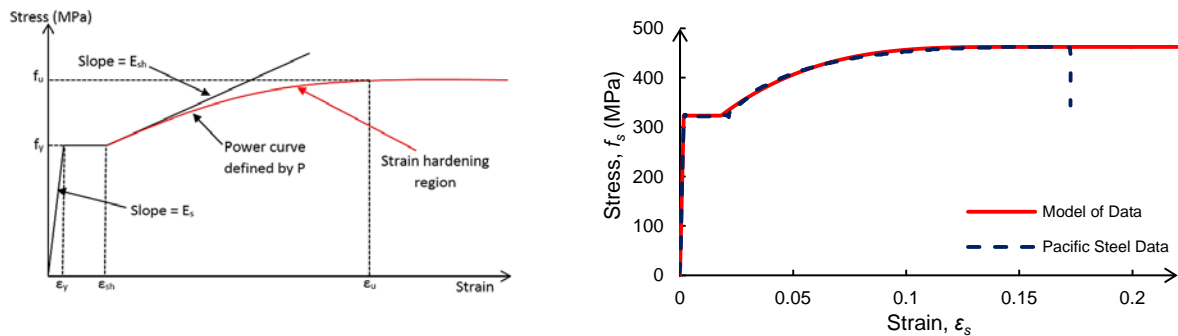


**Figure 1. Steel stress-strain relationship used for this study: (a) Schematic showing the Mander (1984) model parameters required; (b) example of the steel model applied to actual test data from Pacific Steel.**

In Figure 1(a),  $f_y$  is the yield stress,  $f_u$  is the ultimate stress,  $\epsilon_y$  is the yield strain,  $\epsilon_u$  is the ultimate strain,  $\epsilon_{sh}$  is the strain at the onset of strain-hardening, and  $P$  is a response variable used to define the extent of the strain hardening which is modelled as a power curve starting at  $(\epsilon_{sh}, f_y)$  and ending at  $(\epsilon_u, f_u)$ .  $P$  is therefore related to the strain hardening modulus,  $E_{sh}$ .

Test data files supplied by Pacific Steel contained raw measurements of load and displacement. Each model parameter was extracted from the individual data files using a set of MATLAB<sup>®</sup> codes (written by the authors) to be used later for the moment-curvature analysis. This approach ensures the relationships between the yield stress, ultimate stress and the strain hardening curve are reasonably accurate. Although more samples may be generated using Monte Carlo simulations, the six variables considered here are not independent and simulations can potentially lead to unrealistic stress-strain curves.

$E_s$  of 200 GPa was assumed to be representative for all the steel test data. Some test results were significantly less than 200 GPa, which is attributed to grip slip of the deformed bar in the test set-up. One difficult aspect of deducing the model behaviour was determining the onset of the strain hardening curve. The value of  $\varepsilon_{sh}$  significantly affects the shape of the power curve, thus visual inspection of the test data was required to modify the value of  $\varepsilon_{sh}$  to improve the modelled behaviour. An example of the model verification for the reinforcing steel is shown in Figure 1(b) where the model is used to represent the actual stress-strain curve. The sudden drop of stress at the end of the actual curve is due to the termination of the tension test once the ultimate strength is reached (not a material property of the reinforcing steel).

Table 1 summarises results from the test data for D20, D25 and D32 samples, as these are common deformed bar sizes used in RC beams and columns. Table 2 presents a summary of the mean model parameters that were deduced from the test data. The values presented here also meet the requirements for the characteristic mechanical properties that are specified in the Steel Reinforcing Materials Standard, NZS4671:2001. The results are close to the maximum allowable ratio of  $f_u/f_y$ , is 1.50, thus indicating there is a significant amount of strain hardening.

**Table 1. Pacific Steel tension test data (MPa).**

Parameter	Overall	D20	D25	D32	
$f_y$	Lower 5 <sup>th</sup> %	317	316	327	314
	Mean	336	334	337	326
	Upper 95 <sup>th</sup> %	359	357	347	340
$f_u$	Lower 5 <sup>th</sup> %	451	450	472	464
	Mean	475	473	490	478
	Upper 95 <sup>th</sup> %	505	506	505	498
# Samples	100	61	20	19	

**Table 2. Summary of mean model parameters.**

Parameter	Overall	D20	D25	D32
$f_y$ (MPa)	333	334	337	326
$f_u$ (MPa)	477	473	490	478
Ratio $f_u/f_y$	1.43	1.42	1.45	1.47
$\varepsilon_y$	0.0017	0.0017	0.0017	0.0016
$\varepsilon_u$	0.1487	0.1482	0.1522	0.1465
$\varepsilon_{sh}$	0.0185	0.0197	0.0168	0.0161
$P$	3.33	3.33	3.44	3.24

### 3.2 Concrete properties

The stress-strain relationship for confined concrete was modelled based on Mander et al. (1988), as shown in Figure 2. Concrete crushing and spalling strains of the unconfined concrete was taken to be 0.003 and 0.006, respectively (Allington 2003). The transverse reinforcement configuration is assessed when determining the ultimate compressive stresses and strains that the confined concrete may develop. The ultimate compressive strain of the confined concrete,  $\varepsilon_{cu}$ , is limited by the first fracture of the transverse reinforcement (Mander et al. 1988), as defined by Equation 1;

$$\varepsilon_{cu} = 0.004 + \frac{1.4\rho_{st}f_{yt}\varepsilon_{su}}{f_{cu}} \quad (1)$$

where  $\rho_{st}$  is the transverse reinforcement ratio,  $f_{yt}$  is the lower characteristic yield strength of the transverse reinforcement,  $\varepsilon_{su}$  is the ultimate tensile strain of the transverse reinforcement and  $f_{cu}$  is the ultimate compressive strength of the confined concrete.

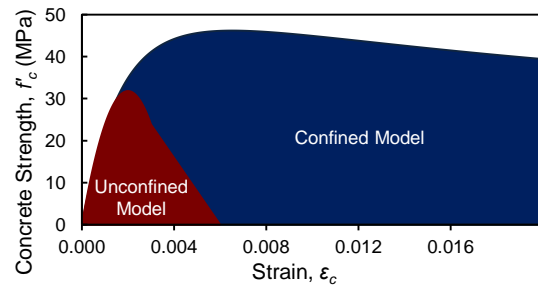


**Figure 2. The confined and unconfined concrete model developed by Mander et al. (1988).**

Allington (2003) illustrated that the confined concrete area is reduced in RC columns with large axial loads due to the arching effect between the restrained longitudinal bars. This arching effect was ignored for the column section analysis completed in this study (presented in a later section) and the entire area inside the stirrups is assumed to be confined. This assumption is reasonable as magnitude of axial loading is relatively low and potential plastic hinge regions have sufficient transverse reinforcement. It is noted that this simplifying assumption may result in a larger column moment capacity compared to the case where the arching effect is considered. For RC beams, the entire concrete was assumed to be unconfined due to the relatively large arching effect between top and bottom longitudinal bars.

Concrete strengths with a range between 25 and 40 MPa were analysed as a representative of the typical structural concrete strength used in design. For this study, the overstrength of concrete was defined as  $[f'_c + 15]$  according to NZS3101:2006 to account for increases in strength due to ageing of the concrete and higher supplied strength than is specified by the designer. Recent material testing from Christchurch buildings found that higher in-place concrete strengths may have that influenced the performance of RC buildings following the 2010-2011 Canterbury Earthquakes (Bull 2012).

### 3.3 Section Properties

The longitudinal and transverse reinforcement configurations for RC beam and column sections were designed according to the ductile detailing requirements in NZS3101:2006. The following subsections describe the variables of the moment-curvature section analysis.

#### 3.3.1 Section geometry

The overstrength factor was evaluated for beam and column sections with varying section dimensions. Beam dimensions ranged between 500-700 mm and 500-1000 mm for the section width and depth, respectively, and column dimensions ranged between 400-800 mm along each side. For beam sections, the depth was always greater than or equal to the width. Symmetrical column sections were used as this helped simplify the analysis. Rectangular sections were used to simplify the computation required for the moment-curvature analysis. In practice, it is important that effective flanges of T-shaped sections are appropriately considered when determining overstrength actions.

#### 3.3.2 Longitudinal reinforcement

Only D20, D25 and D32 bars were used for the longitudinal reinforcement as these are most commonly used for the design of ductile beams and columns in NZ. The number and size of these deformed bars was adjusted to meet the minimum and maximum quantities for the flexural tension reinforcement (to ensure ductility and avoid crushing failure). In columns sections, one layer of reinforcement was used around the perimeter.

#### 3.3.3 Transverse reinforcement

Sections were designed to meet the transverse reinforcement requirements for confinement, anti-buckling and minimum shear capacity. Grade 500 stirrups (HR10s) were arbitrarily adopted as the transverse reinforcement in all column sections.

#### 3.3.4 Applied axial loads

Seismic resistant columns in NZ are typically designed for low axial load ratios to ensure sufficient ductility. Axial load ratios between 0 and 0.3 were used to accurately determine the overstrength behaviour of ductile RC columns.

### 3.4 Material Behaviour under Cyclic Loading

Earthquake-induced ground shaking causes structures to undergo cyclic loading. The effect of cyclic loading on the RC sections was considered in this study in terms of the cyclic material response.

#### 3.4.1 Cyclic concrete behaviour

Mander (1984) showed the monotonic stress-strain curve provides an envelope to the cyclic loading response. No modification was made to the monotonic stress-strain models to account for cyclic effects in this study.

#### 3.4.2 Cyclic steel behaviour

Cyclic loading may cause the reinforcing steel to undergo large inelastic strains. Figure 3 illustrates that cyclic loading of RC beams and columns has a non-linear response at strains below the yield strain (commonly known as the Baushinger effect). Figure 3(a) shows the flexural tension steel in RC beams is unlikely to experience large inelastic compressive strains during cyclic load reversals. This study chose therefore to adopt the monotonic stress-strain curve as an envelope for the cyclic response of RC beams that were analysed. For RC columns, the effect of axial loading causes the section to experience large inelastic compressive strains in the reverse cycle, as shown in Figure 3(b). To

account for inelastic compressive strains, this study adopted a pseudo-cyclic approach in attempt to model the cyclic behaviour by shifting the origin of the monotonic envelope. Figure 4 schematically illustrates the method of shifting the monotonic envelope that was developed by Presland (1999).

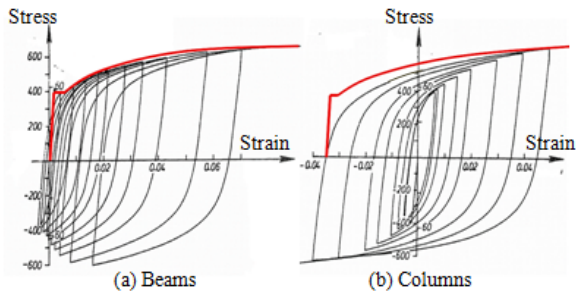


**Figure 3. Experimental stress-strain behaviour of beams (left) and columns (right) subjected to cyclic loading (Paulay and Priestley 1992).**

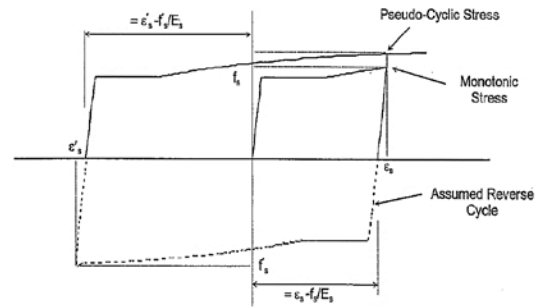


**Figure 4. The shifted monotonic stress-strain curve for the pseudo-cyclic loading (Presland 1999).**

The shift function assumes the behaviour of the section in compression is equal and opposite to the tension behaviour, which is indicated by the symmetry of the experimental results shown in Figure 3(b). To account for inelastic compressive strains, the monotonic stress-strain curve is shifted by the corresponding residual plastic strain, which is defined in Equation 2:

$$\text{Shift} = \varepsilon'_s - \frac{f'_s}{E_s} \quad (2)$$

where  $\varepsilon'_s$  is the maximum steel compression strain,  $f'_s$  is the maximum steel compression stress and  $E_s$  is the Elastic Modulus (200 GPa)

### 3.5 Curvature Ductility

The yield curvature ( $\phi_y$ ) definition was based on first yield of the longitudinal reinforcement. Material and flexural overstrength values were calculated at a curvature ductility of  $5\phi_y$ ,  $10\phi_y$ ,  $20\phi_y$  and  $25\phi_y$ . NZS3101:2006 determines the overstrength based on a curvature ductility of 20. This is commonly accepted as the ultimate limit state (ULS) curvature limit for reversing plastic hinges in RC structures.

## 4 ANALYSIS METHOD

### 4.1 Moment-curvature model development

A moment-curvature fibre section analysis tool '*MC analysis*' was developed using MATLAB<sup>®</sup> to determine the flexural and material overstrength factors for RC sections. The tool required various inputs including section geometry, bar size and number of bars. By setting the neutral axis and curvature of a section, the strains across the section can be calculated. *MC analysis* divided each section into 100 horizontal strips. Calculated strains were then taken as inputs to the steel and concrete models (described earlier in Section 3) to extract the respective steel and concrete stresses. The force components in each strip were then calculated. The initial neutral axis was iterated upon until convergence of section force equilibrium was achieved and the corresponding moment capacity was determined.

For each permutation of the analysis, the curvature of the section was incrementally increased to generate the moment-curvature section response. Two curvature increments were used to improve the accuracy and efficiency of the programme. Smaller increments were initially used as the moment capacity rapidly increases and larger increments were used in the post-yield range. Section failure was defined by either the longitudinal reinforcement reaching the ultimate tensile strain, or when the confined concrete reached the ultimate compression strain.

After *MC analysis* was validated for RC beam sections, the tool was further developed for the additional complexities in modelling RC columns (such as confinement, axial loading and cyclic loading). Separate fibres for confined and unconfined cover concrete meant that cover spalling could be modelled along section perimeter. The function files used for force-equilibrium and iterative neutral axis position were modified to include axial loading. A pseudo-cyclic function (as detailed in Section 3.4.2) was added to complete reverse cycles of the section to determine the compressive strains,  $\epsilon'_{s}$ , experienced under cyclic loading. The elastic recovery was deducted from this strain giving the corresponding shift of the curve for the tension stress-strain relationship. If the reinforcement remained in the elastic range then no shift was applied.

### 4.2 Model verification

The accuracy of *MC analysis* was first validated by assessing the monotonic section response of RC beams in comparison with simple hand calculations and with moment-curvature outputs from other software. Figure 5(a) shows an example the results obtained for a 400 mm by 600 mm RC beam section in comparison with results from Response-2000 (Bentz and Collins 2001), Sap-2000 (Computers and Structures 1998) and Cumbia (Montejo and Kowalsky 2007).

Verification of the results for column sections was conducted for a range of different axial loads. As expected, the moment-curvature response exhibited a decrease in ductility at higher axial loads. Figure 5(b) presents an example of the comparison with other software for a given section with an axial load ratio of 0.2. The results comparison for RC columns was affected by slight variations between material models that were used for each software tool. Confined concrete was not modelled in Response-2000 and hence Figure 5(b) shows the most significant decrease in the post-peak moment capacity. Results obtained from Cumbia and from fibre-section modelling in OpenSees (2012) were particularly useful in validating the monotonic response column sections predicted by the tool *MC analysis*.

To verify the pseudo-cyclic function, laboratory specimens tested by Li et al. (1994) and the pseudo-cyclic moment-curvature response from Allington (2003) were used. Results shown in Figure 5(c) indicate that *MC analysis* provides good prediction compared to the actual measured behaviour.

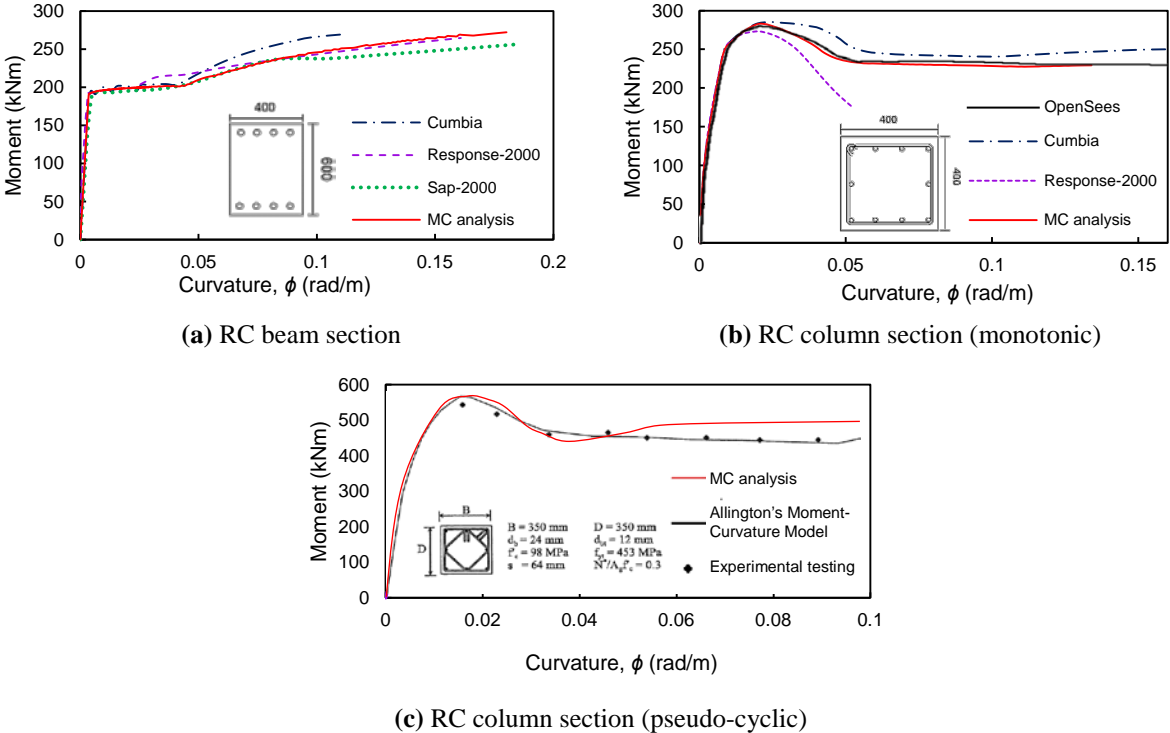


Figure 5. Validation of ‘MC analysis’ using different software tools.

## 5 RESULTS AND DISCUSSION

At a given curvature  $\phi_i$ , the material overstrength value  $\phi_{o,fy}$  was determined by dividing the reinforcing steel stress by the nominal yield stress of 300 MPa, not the mean yield stress found from tension tests, i.e.  $\phi_{o,fy} = f_{s,i}/300$ . Similarly, at a particular curvature the flexural overstrength factor  $\lambda_o$  was determined by dividing the section moment capacity by the nominal moment capacity that was calculated as per the method in NZS3101:2006, i.e.  $\lambda_o = M_{o,i}/M_n$ . The flexural and material overstrength factors were calculated based on combinations of different axial load ratios, concrete strengths, section shapes, reinforcement configurations and stress-strain properties. Overstrength factors were evaluated based on the 95<sup>th</sup> percentile of the normally distributed results to ensure a low probability of exceeding the overstrength capacity of the member.

### 5.1 Beam results

The material overstrength values obtained from 2520 monotonic beam analyses, at different curvature ductility's, are displayed in Table 3. Flexural overstrength values are displayed in Table 4. The flexural and material overstrength factors are very similar as the reinforcing steel material response dominates the flexural behaviour of beam sections, particularly as the modelled concrete behaviour did not account for confinement (explained previously in Section 3.2). The increase in overstrength at  $15\phi_y$  is due to the onset of strain hardening. Based on the 95th percentile values at  $20\phi_y$ , the analysis indicates  $\phi_{o,fy} \approx 1.46$  and  $\lambda_o \approx 1.47$ , respectively.

**Table 3. Results for beam material overstrength factor,  $\phi_{o,fy}$ .**

Curvature Ductility	Lower 5 <sup>th</sup> %	Mean	Upper 95 <sup>th</sup> %	Std.Dev.
5	1.05	1.11	1.18	0.04
10	1.07	1.15	1.24	0.05
15	1.16	1.26	1.36	0.06
20	1.25	1.35	1.46	0.07
25	1.32	1.42	1.53	0.07

**Table 4. Results for beam flexural overstrength factor,  $\lambda_o$ .**

Curvature Ductility	Lower 5 <sup>th</sup> %	Mean	Upper 95 <sup>th</sup> %	Std.Dev.
5	1.06	1.12	1.19	0.04
10	1.09	1.17	1.26	0.05
15	1.19	1.28	1.38	0.06
20	1.26	1.36	1.47	0.07
25	1.29	1.41	1.53	0.08

Values of  $\lambda_o$  obtained from *MC Analysis* could be slightly low due to the decision to model the core concrete using unconfined stress-strain behaviour (discussed in Section 3.2). The section response in Figure 5(a) shows a reasonable match with Response-2000 and Sap-2000, although the Cumbia results are shown to be slightly higher. The section analysis performed in Cumbia modelled the core concrete with the Mander (1984) confined concrete model. As such, the moment values obtained from Cumbia shown in Figure 5(a) are slightly higher than the outputs from other software tools.

### 5.2 Column results

The material overstrength values for 4656 pseudo-cyclic column analyses are displayed in Table 5. In general, material overstrength values were lower (compared with beams) as less steel strain hardening occurs when the axial and concrete compressive forces have a larger influence on the section moment capacity.

**Table 5. Results for column material overstrength factors,  $\phi_{o,fy}$ .**

Curvature Ductility	Lower 5 <sup>th</sup> %	Mean	Upper 95 <sup>th</sup> %	Std. Dev
5	1.11	1.11	1.18	0.04
10	1.14	1.14	1.21	0.05
15	1.24	1.24	1.32	0.06
20	1.33	1.32	1.41	0.06
25	1.39	1.39	1.49	0.06

**Table 6. Results for column flexural overstrength factor,  $\lambda_o$ .**

Curvature Ductility	Lower 5 <sup>th</sup> %	Mean	Upper 95 <sup>th</sup> %	Std. Dev
5	1.10	1.36	1.58	0.14
10	1.04	1.31	1.59	0.17
15	1.06	1.31	1.61	0.17
20	1.06	1.33	1.65	0.18
25	1.04	1.36	1.70	0.20

Upper characteristic values for  $\lambda_o$  are shown in Table 6 to be relatively large. This is likely due to the conservative manner in which  $\lambda_o$  was calculated as the reference value of the nominal design capacity (using the NZS3101:2006 method) is determined without accounting for the effects of concrete confinement. However, confined concrete significantly increases the section capacity that was modelled in *MC analysis*. Based on  $20\phi_y$ , the analytical results for column sections indicate that  $\phi_{o,fy} \approx 1.41$  and  $\lambda_o \approx 1.65$ , respectively.

Table 7 shows the influence of axial load on both  $\phi_{o,fy}$  and  $\lambda_o$ . For the same curvature values of  $20\phi_y$ , increasing the axial load results in a minor decrease in the steel strain ductility that develops, meaning there is a slight reduction in the amount of strain hardening and hence there is a minor decrease in the values of  $\phi_{o,fy}$ . Comparing the two different metrics, the values of  $\phi_{o,fy}$  are reasonably consistent whilst  $\lambda_o$  varies significantly with axial load. This is partly due to (i) how the nominal moment capacity is calculated and used as a reference value for  $\lambda_o$ , and (ii) the extent and proportion at which axial load affects the confined concrete and steel material responses. The large variability between values of  $\lambda_o$  indicates the uncertainty in determining overstrength actions of ductile columns and it is therefore inappropriate to use  $\lambda_o$  as a single metric for quantifying overstrength behaviour. In contrast, the results indicate that overstrength actions can be reliably determined based on separate consideration of the ‘likely maximum material strength’ whilst still using relatively consistent values of  $\phi_{o,fy}$ , and by using  $[f'_c + 15]$  for the concrete compressive strength (discussed previously in Section 3.2).

**Table 7. The 95th percentile overstrength factors in columns at  $20\phi_y$**

Axial Load ratio	Material, $\phi_{o,fy}$	Flexural, $\lambda_o$
<b>0</b>	1.43	1.72
<b>0.1</b>	1.41	1.55
<b>0.2</b>	1.41	1.48
<b>0.3</b>	1.40	1.41

## 6 CONCLUSIONS AND RECOMENDATIONS

Tension test data for Grade 300E reinforcing steel was supplied by Pacific Steel to evaluate the implications of the stress-strain behaviour on the overstrength flexural capacity of RC structural components. A moment-curvature sectional analysis tool ‘*MC analysis*’ was developed to analyse and quantify the overstrength behaviour for 7176 RC beam and column sections. *MC analysis* was verified using hand calculations, a range of computer software and experimental data.

Outputs of the analysis indicates that, for a curvature ductility of 20 and using the 95th percentile values, the material overstrength factor is 1.46 (mean of 1.35) for beams and 1.41 (mean of 1.32) for columns. Increased section moment capacities were mainly due to higher than average steel yield stresses compared to the specified nominal value of 300 MPa, and a large ratio of  $f_u/f_y$  indicating significant strain hardening. The flexural overstrength of beams was approximately similar to the material overstrength of the reinforcing steel, whereas the flexural overstrength of columns was dominated by the material behaviour of both the reinforcing steel and the confined concrete.

The material overstrength value  $\phi_{o,fy}$  specified for Grade 300E in NZS3101:2006 is 1.25. Previous research, and earlier versions of the standard, specified the use of a single flexural overstrength factor applied to the nominal moment capacity (i.e.  $M_o = \lambda_o M_n$ ). Parametric analysis from this study found that overstrength calculations based on the material overstrength value  $\phi_{o,fy}$  for the reinforcing steel is a more accurate and reliable method. The outcomes of this specific study suggest that  $\phi_{o,fy}$  of 1.25 is too low and a more appropriate value may be between 1.35-1.45. Recent draft changes in Amendment 3 of NZS3101:2006 increased  $\phi_{o,fy}$  to 1.35 (the same value is specified for Grade 500E steel). Some of the analysis results from this research provide good agreement with this proposed change.

The application of the analysis completed is limited by the sample size of steel data used and the number of sections analysed. Overstrength values determined in this study are slightly larger than those found in previous research, which will depend on the manufacturer's source material and may possibly be due to modern changes in the metallurgical composition to ensure a more ductile product. Changes in the metallurgical composition may ultimately affect the overstrength actions in RC structures. A recommendation of this research is to repeat and update this analysis procedure to re-evaluate the material overstrength factor that is considered for future structural design.

## 7 ACKNOWLEDGEMENTS

This research was completed by the first two authors as an undergraduate project at the University of Canterbury. Mr Bruce Roberts from Pacific Steel is acknowledged for his assistance with supplying tension test data on Grade 300E reinforcing steel samples.

## 8 REFERENCES

- Allington, C.J. 2003. Seismic performance of moment resisting frame members produced from lightweight aggregate concrete, *PhD thesis, University of Canterbury, Christchurch*.
- Andriono, T. & Park, R. 1986. Seismic design considerations of the properties of New Zealand manufactured steel reinforcing bars. *Bulletin of the New Zealand National Society for Earthquake Engineering*, 19(3): 213-246.
- Bentz, E. & Collins, M.P. 2001. Response-2000, University of Toronto.
- Brooke, N. & Ingham, J. 2011. The Effect of Reinforcement Strength on the Overstrength Factor for RC Beams. *Paper presented at the Proceedings of the Ninth Pacific Conference on Earthquake Engineering Building an Earthquake-Resilient Society*.
- Bull, D.K. (2012). The performance of concrete structures in the Canterbury earthquakes: *Lessons for concrete buildings*, Structural Engineers Association of California (SEAOC) Convention, Santa Fe, NM.
- Bull, D.K. & Allington, C. 2003. Overstrength Factor for Pacific Steel Micro-Alloy Grade 500 Reinforcement: April 2002. *Journal of the Structural Engineering Society New Zealand*, 16(1): 52-53.
- Computers and Structures Inc. 1998. SAP2000 – The three dimensional static and dynamic finite element analysis and design of structures. Berkeley, California.
- Mander, J.B. 1984. Seismic design of bridge piers. Research Report 84-2, Department of Civil Engineering, University of Canterbury, Christchurch, 483pp.
- Mander, J.B., Priestley, M.J. & Park, R. 1988. Theoretical stress-strain model for confined concrete. *Journal of structural engineering*, 114(8): 1804-1826.
- Montejo L.A. & Kowalsky M.J. 2007. CUMBIA – Set of codes for the analysis of reinforced concrete members, *Technical Report No. IS-07-01*, North Carolina State University.
- OpenSees. 2012. The Open System for Earthquake Engineering Simulation software, version 2.4.1. Pacific Earthquake Engineering Research Centre.
- Paulay, T. & Priestley, M. J. N. 1992. Seismic design of RC and masonry buildings. New York, N.Y.: Wiley.
- Presland, R.A. 1999. Seismic performance of retrofitted RC bridge piers, PhD thesis, University of Canterbury, Christchurch.
- Standards New Zealand. 1995. *Concrete Structures Standard*, NZS3101: Part1: 1995.
- Standards New Zealand. 2006. *Concrete Structures Standard*, NZS3101: Part1 & Part 2: 2006.
- Standards New Zealand. 2001. *Steel Reinforcing Materials Standard*, NZS4671:2001.